Ilkogretim Online - Elementary Education Online, 2021; Vol 20 (Issue 1): pp. 6080-6088
http://ilkogretim-online.org
doi: 10.17051/ilkonline.2021.01.634

Analysis And Development Of Fidelity And Regularization Learning Based Image Restoration Techniques

Amit Sharma Assistant Professor Department of Computer Science and Engineering Sir Chhotu Ram Institute of Engineering & Technology C.C.S. University Campus, Meerut.

Praveen Panwar Assistant Professor Department of Information Technology Sir Chhotu Ram Institute of Engineering & Technology C.C.S. University Campus, Meerut.

Laxmi Shankar Singh Assistant Professor Department of Information Technology Sir Chhotu Ram Institute of Engineering & Technology C.C.S. University Campus, Meerut.

Rupal Chaudhary Assistant Professor Department of Computer Science and Engineering Sir Chhotu Ram Institute of Engineering & Technology C.C.S. University Campus, Meerut.

Abstract—Image restoration, which seeks to restore a damaged observation's underlying clean image, is a basic challenge in low level vision. The majority of extant non-blind restoration approaches are predicated on the knowledge of a specific deterioration model. Due to the fact that the deterioration process can only be partly understood or correctly represented, photos may not be recovered completely. Two notable instances of such tasks are the elimination of rain streaks and picture deconvolution using inaccuracy blur kernels. Although an input picture may be divided into a scene layer and a rain streak layer for the purpose of rain streak removal, there is no clear formulation for modeling rain streaks and their composition with the scene layer. Due to the estimate error generated by the blur kernel in blind deconvolution, the following non-blind deconvolution step does not adequately recover the latent picture. In this article, we offer a principled approach for picture restoration using a partly known or erroneous deterioration model inside the maximum a posteriori framework.

Key Terms—Image restoration, rain streak removal, blind deconvolution, task-driven learning.

I. INTRODUCTION

Image processing is a technique in which we improve the sensor data (raw pictures) placed on various artifacts of life for different applications. As artifacts are clearly visible in comparison with the original sensed image, this results in higher quality.

- Median Filter
- Adaptivek Filter
- Linear Filters
- IBD (Iterative Blind De-convolution) Method
- Non Negative and Support Constraints Recursive Inverse Filtering (NAS-RIF)

- Super-Resolution Restoration
- Deconvolution
- Block Matching
- Wiener Filter
- Deconvolution using Regularized Filter
- Lucy Richardson Algorithm Techniques

Furthermore, we define the regulator by a variety of nonlinear penalty functions for clean-image filters. The SFARL model is formulated as a bi-level problem in order to optimize the inner task by a gradient descent scheme and the training data will provide insight into phase-specific parameter. The effect and visual quality of the SFARL model are demonstrated by experimental results on image deconvolution and rain streak removal.In addition, the SFARL model can also be used to learn the proper trustworthiness term to improve visual perception metrics and to obtain results with better visual quality for image restauration with a specific degradation method e.g. non-blind Gaussian Denoising.

Similar parametric terminology has been used for the layout of natural images in the CSF[3], TNRD [12] and UNET [13] models, and classification is being used for the purposes of restoration. However, this degradation is believed to be understood precisely, and hence the term fidelity, e.g., '2 Norm for deconvolution with the soil-truth kernel, is explicitly defined. However, this degradation is believed to be understood precisely, and hence the term fidelity, e.g., '2 Norm for deconvolution with the soil-truth kernel, is explicitly defined. However, the degradation process is usually partially known in practical applications , for instance inaccurately estimated blurry kernel, rain layer and background layer separation and the combination of multiple degrees. Our SFARL model is, in contrast, designed to provide a theory of restoration in which the term trust is versatile and easily adapted to the process of partially understood degradation.

II. LITERATURE SURVEY

Precisely whitening kernels and removing rain stripes were proposed for various visual tasks.

We employ the nonorthogonal multiuser access (NOMA) technique to handle large numbers of devices [9] and nonorthogonal resource allocation.

[19] investigates Massive connection was examined using information theoretical capacity. Thesis [9] examined NOMA's difficulties and prospects. a CS-based model [10, 20] revealed the sparsity activity pattern. More radio access points in IoT networks [18]support large device connection, allow low-latency mobile apps, and increase network capacity.

In this paper, we look at the intermittent device activity A recent connection between the BS and an active device If the orthogonal signature sequence chosen by the active device is not utilised by other devices. [15] studied random access in cellular networks. Thesis [16] explored dealing with the enormous number of gadgets. This approach caused vast numbers of devices to collide.

Various techniques are available:

1. Rain streak removal

2. Imaged econvolution with inaccurate blurkernels
3. Discriminative Image Restoration
4. Noise Modeling

III. FORMULATION & METHODOLOGY

A. Proposed algorithm

We study image restoration situations when the degrading model is unknown but there exist training pairs of degraded and true pictures. To address these issues, we employ a flexible model to express the fidelity term produced by incomplete or incorrect breakdown. Based on training data, a task-driven learning strategy may attain task-specific trustworthiness.

We discover image restoration issues when the degradation pattern is partly or incorrectly detected, although training pairs of degraded and genuine images exist. So we utilise a flexible model to explain the honesty term caused by an inaccurate breakdown. For a given issue, a task-driven learning technique may be designed.

B. Fidelity Term

The fidelity name is used to describe the spatial dependence of the residual imager = g(x;B)+n. For example, "2-norm and" 1-norm "cannot model the complex distribution for the residual image r. For one thing, the common explicit formulation. Based on the assumption i.e. that current approaches to noise modeling, for example, GMM[37] and Mo EP [6], are also not readily adaptable in terms of fidelity to model spatial dependence. The residual r, on the other hand, is typically space-dependent and complexly distributed.Motivated bythe successof discriminative regularizationlearning [3], [11], we also use a set of linear filters $\{p_i\}_{i=1}^{N}f$ with diverse patterns to model the spatial dependency in g(x; B). Moreover, due to the effect of n and its combination with g(x; B), the filter responses $\{r \otimes p_i\}_{i=1}^{N}f$ remain of complex distribution. Therefore, a set of non-linear penalty functions $\{D_i\}_{i=1}^{N}f$ is further introduced to characterize the distribution of filter responses.

To sum up, we suggest a principled residual modelling in the fidelity term as follows,

$$F(x) = \lambda \sum_{j=1}^{N} \sum_{i=1}^{N_f} D_i\left((P_i \otimes (Ax - y))_j\right), \qquad (9)$$

C. Regularization Term

To boost modelling capability on image prior, the regularisation term is additionally parameterized as

$$R(x) = \sum_{j=1}^{N} \sum_{i=1}^{Nr} R_i\left((f_i \otimes x)_j\right), \qquad (10)$$

CS FARL Model

The fidelity and regularisation terms parameters must be defined for a given picture restoration project. There are too many variables involved in F(x) and R(x) for the right values to be determined manually. Learn task-specific characteristics like as fidelity and regularisation in this study.

Denote a training set of S samples by $\{y_s, x_s^{gt}\}_{s=1}^{S}$ s=1,where $y_s$is the s-th degraded image and x_s^{gt} is the corresponding ground truth image. The parameters $\ominus = \{\ominus_f, \ominus_r\}$ can be learned by solving the following bi-level optimization problem.

$$\begin{aligned} &\min_{\Theta} \mathcal{L}(\Theta) = \sum_{s=1}^{S} \ell\left(\mathbf{x}_s^*, \mathbf{x}_s^{gt}\right) \\ &\text{s.t. } \mathbf{x}_s^* = \arg\min_{\mathbf{x}\in\mathcal{X}} \sum_{j=1}^{N}\sum_{i=1}^{N_r} \mathcal{R}_i\left((\mathbf{f}_i \otimes \mathbf{x})_j\right) \\ &\quad +\lambda \sum_{j=1}^{N}\sum_{i=1}^{N_f} \mathcal{D}_i\left((\mathbf{p}_i \otimes (\mathcal{A}\mathbf{x}-\mathbf{y}_s))_j\right), \end{aligned} \tag{11}$$

As the loss function, we employ the visual perception measure, e.g., negative SSIM [54].

$$\boldsymbol{\ell}(\mathbf{x}, \mathbf{x}^{\mathbf{gt}}) = -\mathbf{SSIM}(\mathbf{x}, \mathbf{x}^{\mathbf{gt}}) \tag{13}$$

There are two reasons for the use of negative SSIM. On the one hand, SSIM is well known to be closely linked to visual expectations of image quality and the visual quality of the restoration result is expected to benefit from the reduction of negative SSIM. In contrast, the negative log-likeness is not an optimized fidelity term when using the negative SSIM loss even for image restoration with a specific degradation procedure. The residual model (9) can therefore be used to learn right trustworthiness from training data to either de-convolve images with incorrect blurs, to erase rain streaks or to denoise Gaussian. Furthermore, the experimental data confirm the efficacy of negative SSIM a SSIM andresidual modeling in terms of both visual qualityand perception metric.

D. Sfarl training

In this section, we present an iterative solution to the internal task of the two-tier problem of optimisation. The SFARL model can then be used for training with a parameterized gradient-based algorithm. The SFARL model is trained via the sequence of greedy algorithm 2 testing and algorithm 3 joint refining. Finally, gradient derivations for greedy and end-toend training are seen.

E. Iterative Solution

To solve the problem of optimization we use ADAM [55] (14). Consequently, in (15) we will present the solution parameterisation and calculate gradients for the greedy and end-to end learning processes.

F. Training Procedure

In the light of the training dataset, the SFARL testing is conducted sequentially as an algorithm 2, as well as joint modifications as an algorithm 3. Algorithm 1 lists the inference of model parameters given by SFARL which are recorded for retrospective propagation during training for all intermediate results.

Algorithm 1 SFARL

Input: Current result $\mathbf{x}^0$, degraded image $\mathbf{y}$, degradation operator $\mathcal{A}$, model parameters $\{\Theta^t\}_{t=1}^T$
Output: Restoration results $\mathbf{x}$
1: **for** $t = 0$ to $T-1$ **do**
2: Compute $\mathbf{x}^{t+1}$ using (15)
3: **end for**
4: $\mathbf{x} = \{\mathbf{x}^1, \mathbf{x}^2, ..., \mathbf{x}^T\}$

Algorithm 2 Greedy Training

Input: Training data $\{\mathbf{y}_i, \mathbf{x}_i^{gt}, \mathcal{A}_i\}_{i=1}^N$
Output: SFARL parameters $\{\Theta^t\}_{t=1}^T$
1: Set stage number T, epoch number E, mini-batch size n, mini-batch number $M = N/n$
2: Initialize: $\{\mathbf{x}_i^0 | \mathbf{x}_i^0 = \mathbf{y}_i\}_{i=1}^N$, $\{\Theta^t\}_{t=1}^T$
3: **for** $t = 0$ to $T-1$ **do**
4: **for** *epoch* $= 1$ to E **do**
5: **for** $m = 0$ to $M-1$ **do**
6: Prepare m-th mini-batch data: $\{\mathbf{y}_i, \mathbf{x}_i^{gt}, \mathcal{A}_i\}_{i=m\times n+1}^{m\times n+n}$
7: Forward samples in m-th mini-batch:

$$\mathbf{x}_i^{t+1} = \text{SFARL}(\mathbf{x}_i^t, \mathbf{y}_i, \mathcal{A}_i, \Theta^{t+1})$$

8: Compute gradients for stage $t+1$: $\frac{1}{n}\sum_i \frac{\partial \ell(\mathbf{x}_i^{t+1}, \mathbf{x}_i^{gt})}{\partial \Theta^{t+1}}$
9: Use Adam to optimize stage $t+1$ parameters Θ^{t+1}
10: **end for**
11: **end for**
12: **end for**

In greedy training $\ominus^{\mathbf{t+1}}$**,** parameters $\{\ominus^{\mathbf{i}}\}_{\mathbf{i=1}}^{\mathbf{t}}$ in previous t stages are fixed, and only gradientsinstage **t+1** are computed and a refed to ADA Malgorithm. In joint fine-tuning, gradients in each stage are computed, and are fed to ADA Malgorithm to optimize the parameters $\{\ominus^{\mathbf{t}}\}_{\mathbf{t=1}}^{\mathbf{T}}$for all the stages.

Algorithm 3 Joint Fine-tuning

Input: Training data $\{\mathbf{y}_i, \mathbf{x}_i^{gt}, \mathcal{A}_i\}_{i=1}^N$, model parameters $\{\Theta^t\}_{t=1}^T$
Output: SFARL parameters $\{\Theta^t\}_{t=1}^T$
1: Set epoch number E, mini-batch size n, mini-batch number $M = N/n$
2: Initialize $\{\mathbf{x}_i^0 | \mathbf{x}_i^0 = \mathbf{y}_i\}_{i=1}^N$
3: **for** *epoch* $= 1$ to E **do**
4: **for** $m = 0$ to $M-1$ **do**
5: Prepare m-th mini-batch data: $\{\mathbf{y}_i, \mathbf{x}_i^{gt}, \mathcal{A}_i\}_{i=m\times n+1}^{m\times n+n}$
6: Forward samples in m-th mini-batch:

$$\{\mathbf{x}_i^1, \mathbf{x}_i^2, ..., \mathbf{x}_i^T\} = \text{SFARL}(\mathbf{x}_i^0, \mathbf{y}_i, \mathcal{A}_i, \{\Theta^t\}_{t=1}^T)$$

7: Compute gradients for each stage: $\{\frac{1}{n}\sum_i \frac{\partial \ell(\mathbf{x}_i^T, \mathbf{x}_i^{gt})}{\partial \Theta^t}\}_{t=1}^T$
8: Use Adam to end-to-end optimize parameters $\{\Theta^t\}_{t=1}^T$
9: **end for**
10: **end for**

IV. SIMULATIONS&RESULT

The proposed SFARL algorithm is evaluated in this section on several restoration tasks, e.g. deconvolution of images with either an inaccurate blurred kernel or several break-ups and removal of rain streak from a given image. SFARL may also be evaluated on Gaussian denoising and the results in additional material have been presented. In our experiments the fidelity and regularization of 7 out of 7 filters is taken. As far as stage number is concerned, we advise to use 10-phase SFARL for image deconvolution and 5-phase SFARL for rainbow removal and gaussi and enoising on a basis of convergence comportment during greedy workouts.

Fig. 2: Visual quality comparison on Levin et al.'s dataset [57].

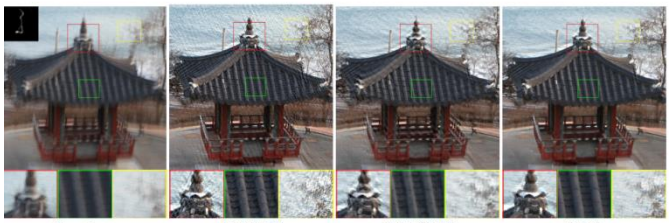

Fig. 3: Deblurring results on real blurry images, in which blur kernels are estimated by Xu and Jia [18].

The SFARL algorithm is evaluated in Figure 2 and 3 against state-of-the-art methods for a synthetic and a real blurred image.

SINGE IMAGE RAIN STREAK REMOVAL

IRCNN works well to diminish fluidity but causes additional degradation to noise effects and induce rounding. SRN is an up-tocurrent network for deep-motion blurring, but still contains visible noise and objects since the malfunction due to future is often worse than fluttering movement. We find that SFARL is therefore in a position to fidelity simulate these various breakdowns. In addition, DCNN will initiate the subnet work deconvolution using opposite kernels, whereas our SFARL is considerably easier to train given a correct training dataset.

The state-of-the-art SFARL algorithms are examined using a synthetic dataset, such as CNN [62] and GMM [24]. The dataset comprises of 12 rainy photos with a left to right direction. Table 3 illustrates the highest SSIM values for each test picture are produced using the SFARL method. Fig. 5 exhibits all the evaluated techniques on a simulated wet photo to erase the rain streak effects.

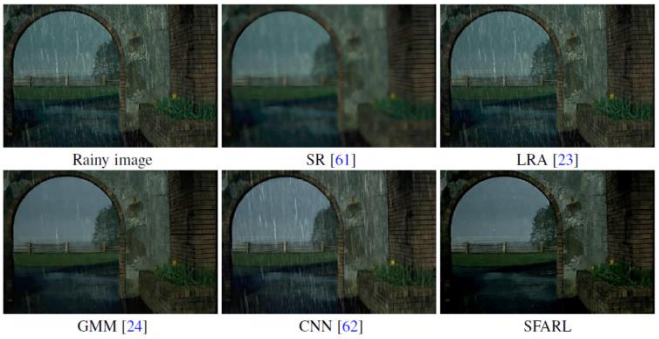

Fig. 5: Rain streak removal results of five evaluated methods on a synthetic image in [24].

There is a significantly better result than other methods with FSARL and GMM algorithms. The product of the GMM method however still has obvious rain streaks, while the SFARL model recovers a clean picture.

Regularization filters are used for the modeling and free transfer of clean images from a generative learning perspective. However, due to the implications of discriminatory learning the SFARL regularization filters are often changed into a specific degradation type. In brief, the general potential for particular behaviors, especially all types of degradation (e.g. deraining and denoting) is rational.

Fig.6: Contrast of visual consistency for the removal of rain strips.

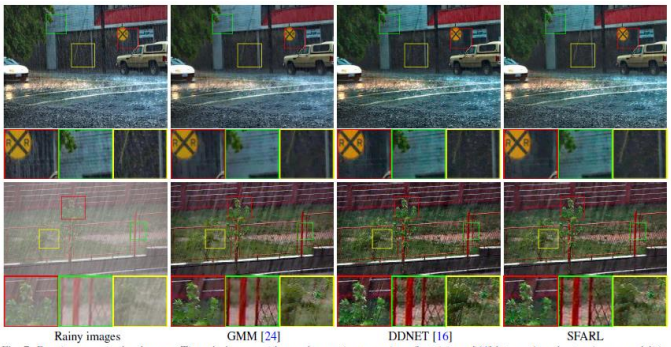

Fig. 7: Results on real rainy images. The rain in second image is very heavy and we first dehaze [64] it to make rain streaks more visible.

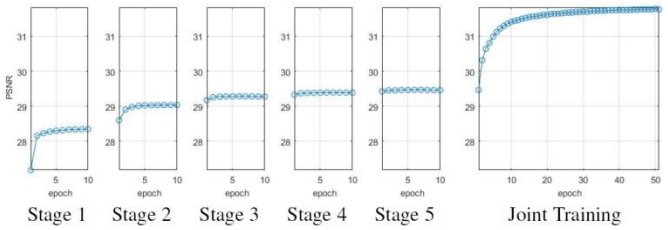

Additionally, we compare the SFARL model to cutting-edge approaches using real-world rainy images. The second photograph of Fig after the storm. We first dehaze[64] the image before using a deraining technique, since 7 is too dense to see the rain strip. For both test pictures, the SFARL algorithm outperforms DDNET[16] and GMM[24]. For genuine rainy photos, the image generation process is complex and cannot be described by either a linear additive or a screen mixing model. Nonetheless, the SFARL model is more effective at modelling and achieving a complicated degradation cycle due to its adaptability in modelling geographically based and extremely complex patterns in terms of realism.

TABLE 4: Comparison of the average PSNR / SSIM values for Rain100L [32] and Rain1400 [16]. DDNET and SFARL are both Rain 1400-compliant and are directly utilised in Rain100L procedures to certify broad capability.

Method	DDNET [16]	SFARL
Rain1400 [16]	29.91/0.9099	31.37/0.9188
Rain100L [32]	29.12/0.9012	29.73/0.9181

CONCLUSION

We present an approach in this paper for managing picture restoration effectively, partly or erroneously. We provide a flexible approach for establishing the fidelity term in order to account for geographical dependency and complicated residual image distributions. The regularisation and simultaneous fidelity learning model is built by incorporating the parameterized regularisation duration. Then, using a collection of degraded pairs of pictures from the ground-to-truth, task and stage-specific model parameters of SFARL may be targeted. Experiments on two picture restoration tasks, photo conversion and rainbow eradication, demonstrate that the SFARL model outperforms advanced approaches in terms of quantitative and visual efficiency. Experiments with Gaussian denoise demonstrate that the SFARL technique successfully improves the visual consistency and visual perception of denoise testing. Our future study will involve the application of the SFARL model to additional restoration jobs and training techniques developed within an unexpected learning framework.

REFERENCES

[1]. Y. Chen and T. Pock, "Trainable nonlinear reaction diffusion: A flexible framework for fast and effective image restoration," IEEE Transactions on Pattern Analysis and Machine Intelligence, vol. 39, no. 6, 2017.

[2]. S. Lefkimmiatis, "Universal denoising networks: A novel cnn architecture for image denoising," in Proceedings of the IEEE Conference on Computer Vision and Pattern Recognition, 2018, pp. 3204–3213.

[3]. X. Fu, J. Huang, D. Z. Y. Huang, X. Ding, and J. Paisley, "Removing rain from single images via a deep detail network," in Proceedings of the IEEE Conference on Computer Vision and Pattern Recognition, 2017.

[4]. J. Pan, D. Sun, H. Pfister, and M.-H.Yang, "Blind image deblurringusing dark channel prior," in Proceeding soft he IEEE Conference on Computer Vision and Pattern Recognition, 2016, pp. 1628–1636.

[5]. J. Pan, Z. Hu, Z. Su, and M.-H. Yang, "l0-regularized intensity and gradient prior for deblurring text images and beyond, "IEEE Transactions on Pattern Analysis and Machine Intelligence, vol. 39, no. 2, pp. 342– 355, 2017

[6]. S. Nah, T. H. Kim, and K. M. Lee, "Deep multi-scale convolutional neural network for dynamic scene deblurring," in CVPR, vol. 1, no. 2, 2017,

[7]. S. Su, M. Delbracio, J. Wang, G. Sapiro, W. Heidrich, and O. Wang, "Deep video deblurring for hand-held cameras," in CVPR, vol. 2, 2017

[8]. J. Pan, W. Ren, Z. Hu, and M.-H. Yang, "Learning to deblur images with exemplars," IEEE Transactions on Pattern Analysis and Machine Intelligence, 2018.

[9]. J. Kim, J. Kwon Lee, and K. Mu Lee, "Accurate image super-resolution using very deep convolutional networks," in Proceedings of the IEEE conference on computer vision and pattern recognition, 2016, pp. 1646– 1654.

[10]. P. Getreuer, I. Garcia-Dorado, J. Isidoro, S.Choi, F.Ong, and P. Milanfar, "Blade: Filter learning for general purpose computational photography," in ICCP, 2018.

[11]. K. He, X. Zhang, S. Ren, and J. Sun, "Deep residual learning for image recognition," in Proceeding soft he IEEE Conference on Computer Vision and Pattern Recognition, 2016, R. T. Tan, J. Feng, J. Liu, Z. Guo, and S. Yan, "Deep joint rain detection and removal from a single image," in

Proceedings of the IEEE Conference on Computer Vision and Pattern Recognition, 2017, pp. 1357–1366.
[12]. K. Zhang, W. Zuo, S. Gu, and L. Zhang, "Learning deep CNN denoiser prior for image restoration," Proceedings of the IEEE Conference on Computer Vision and Pattern Recognition, 2017
[13]. S. Vasu, V. R. Maligireddy, and A. Rajagopalan, "Non-blind deblurring: Handling kernel uncertainty with cnns," in Proceedings of the IEEE Conference on Computer Vision and Pattern Recognition, 2018, pp. 3272–3281
[14]. K. Zhang, W. Zuo, Y. Chen, D. Meng, and L. Zhang, "Beyond a gaussi and enoiser: Residual learning of deep cnn for image denoising," IEEE
[15]. Transactions on Image Processing, vol. 26,
no. 7, pp. 3142–3155, 2017.
[16]. X. Chen, Z. Han, Y. Wang, Q. Zhao, D. Meng, and Y. Tang, "Robust tensor factorization with unknown noise," in Proceedings of the IEEE Conference on Computer Vision and Pattern Recognition, 2016, pp. 5213–5221.
[17]. F. Zhu, G. Chen, and P.-A. Heng, "From noise modeling to blind image denoising," in Proceedings of the IEEE Conference on Computer Vision and Pattern Recognition, 2016
[18]. Schmidt, J. Jancsary, S. Nowozin, S. Roth, and C. Rother, "Cascades of regression tree fields for image restoration," IEEE Transactions on Pattern Analysis and Machine Intelligence, vol. 38, no. 4, pp. 677–689, 2016.
[19]. L. Xiao, J. Wang, W. Heidrich, and M. Hirsch, "Learning high-order filters for efficient blind deconvolution of document photographs," in European Conference on Computer Vision. Springer, 2016, pp. 734– 749
[20]. X. Tao, H. Gao, X. Shen, J. Wang, and J. Jia, "Scale-recurrent network for deep image deblurring," in Proceedings of the IEEE Conference on Computer Vision and Pattern Recognition, 2018, pp. 8174–8182